140

MODELING OF CONJUGATE HEAT TRANSFER IN AN ELECTRICALLY HEATED MICROTUBE

Kevin Cole[1]*, Barbaros Çetin[2]
[1]Mechanical and Materials Engineering W342 Nebraska Hall
University of Nebraska–Lincoln, Lincoln, Nebraska 68588-0626 USA
[2]Microfluidics & Lab-on-a-chip Research Group, Bilkent University, 06800 Ankara, Turkey
*Correspondence author: Phone: +1-402-472-5857, Email: kcole1@unl.edu
Keywords: Wall conduction, microtube, micro heat exchanger, laminar flow, conjugate heat transfer

ABSTRACT
Modeling of conjugate heat transfer in an electrically heated microtube is presneted.To represent the Joule heating, a constant volumetric heat generation is included as a spatially uniform source term in the conduction equation. The heat conduction within the tube wall and the convection within the microtube are analyzed by solving the energy equation. Axial conduction in the fluid and in the adjacent wall is included. The fluid is assumed to be a constant property fluid. The analytic solution is obtained in the form of integrals by the method of Greens functions. Quadrature is used to obtain numerical results for the temperature field within the tube and within the fluid. Effects of the wall thickness and the wall material on the normalized temperature distribution are discussed and future research directions are addressed.

NOMENCLATURE
g	energy generation (W/m^3)
G	steady Green's function (m^{-1})
h	heat transfer coefficient, (W/m^2·K)
j	imaginary number, $\sqrt{-1}$
k_f	thermal conductivity of the fluid (W/m·K)
k_w	thermal conductivity of the wall (W/m·K)
L	axial extent of heated region (m)
N	number of layers in fluid flow
Pe	Peclet number, U r$_f$ /α_f
r	radial coordinate (m)
r_f	radius of fluid flow (tube inner radius) (m)
r_w	outside radius of tube wall (m)
T	temperature (K)
u	local velocity (m/s)

Greek
α	thermal diffusivity (m^2 ·s^{-1})
β	wave number, Eq. (10) (m^{-1})

INTRODUCTION
Channels with a size on the order of micrometers are the key elements of microheat exchangers, microheat sinks, microsensors, and micropower generation systems. As fluid flow and heat transfer occur at the micro-scale, some additional effects such as rarefaction, electro-viscous effects, viscous dissipation, axial

Table 1
Some typical values for the size and material of the microtubes

Reference	Material	d (μm)	D (μm)	Wall thickness (μm)
[6, 7]	Stainless steel	170	1588	709
[6, 7]	Stainless steel	510	1588	539
[6, 7]	Stainless steel	750	1588	419
[8]	Nickel	200	780	290
[8]	Nickel	300	350	25
[8]	Nickel	350	600	125
[8]	Nickel	500	800	150

conduction, etc. need to be considered, which are typically negligible at the macro-scale. From the heat transport point of view, the characteristic time for convection and conduction become comparable at the microscale within the fluid, and the convection term no longer dominates the conduction term in the axial direction. When the Pe number becomes small ($Pe < 50$), axial conduction in the fluid cannot be neglected. The effect of the axial conduction in the fluid becomes more pronounced as Pe decreases. The effect of axial conduction in the fluid on the heat transfer has been studied for both parallel-plate microchannel [1, 2] and microtube [3–5]. Moreover, in macro-channels, the channel wall thickness is small compared to the channel size which leads to negligible heat transfer by conduction through the channel wall (conjugate heat transfer). However, in micro-channels, the thickness of the channel wall becomes comparable to the channel size due to rigidity and fabrication concerns. Nowadays, microtubes out of copper, nickel, aluminum and stainless steel with an inner diameter of $100 - 900\,\mu$m are commercially available. Typically, the wall thickness of the microtubes is ranging between $25 - 700\,\mu$m. Some typical values are given in Table 1. Especially for the small diameter microtubes, the wall thickness is comparable to the inner diameter of the tube (most of the time larger). Therefore, the heat transferred within the channel wall has a contribution to the overall heat transfer. Considering the investigation of the micro-scale effects, there have been many experimental studies regarding fluid flow and heat transfer in microtubes [6, 7, 9–11]. One convenient way to supply the heat to the microtube is to use the Joule heating for metallic microtubes [6, 7, 11]. In this case, voltage is supplied across both ends of the microtube, and electric current is achieved within the metallic wall, which heats the fluid flowing in the microtube. Joule heating is actually a volumetric heat generation mechanism in the tube wall. Therefore, in a rigorous analysis Joule heating needs to be modeled as the volumetric heat generation in the conduction equation. In this study, a conjugate heat transfer in an electrically heated microtube is performed. To represent the Joule heating, a volumetric heat generation is included as a source term in the conduction equation. The heat conduction within the tube

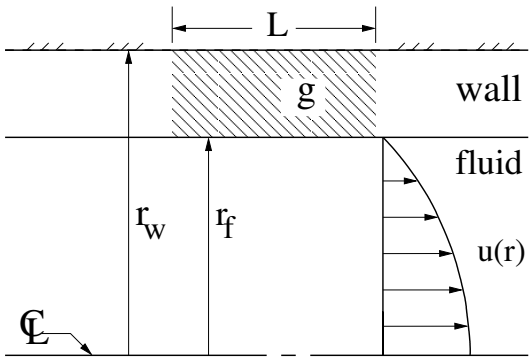

Figure 1
Schematic of the problem

wall and the convection within the microtube are analyzed by solving the energy equation. Axial conduction in the fluid and in the adjacent wall is included. The fluid is assumed to be a constant property fluid. The analytic solution is obtained in the form of integrals by the method of Green's functions. The effects of the wall thickness and the wall material on the normalized temperature distribution are discussed.

ANALYSIS

Temperature Equations: The equations describing the temperature in the circular-tube flow and in the adjacent tube wall are given in this section. The geometry is shown in Fig. 1. The outside wall of the flow channel is heated, and the flow in the tube is fully-developed laminar. The inner radius of the tube is r_f and the outer radius of the tube is r_w. The temperature satisfies the following equations:

$$\text{Wall: } \nabla^2 T_w + \frac{g_o}{k_w} = 0, \quad r_f < r < r_w \tag{1}$$

$$\text{Fluid: } \nabla^2 T_f = \frac{u(r)}{\alpha_f}\frac{\partial T_f}{\partial x}, \quad 0 < r < r_f \tag{2}$$

$$k_w \left.\frac{\partial T_w}{\partial r}\right|_{r=r_w} + hT_w|_{r=r_w} = hT_\infty, \tag{3}$$

$$\left.\frac{\partial T_f}{\partial r}\right|_{r=0} = 0, \tag{4}$$

$$T(x \to \pm\infty, r) \text{ is bounded} \tag{5}$$

with matching conditions between the fluid and solid given by:

$$T_w(r_f) = T_f(r_f), \tag{6}$$

$$-k_w \left.\frac{\partial T_w}{\partial r}\right|_{r=r_f} = -k_f \left.\frac{\partial T_f}{\partial r}\right|_{r=r_f} \tag{7}$$

Heat is added by volume heating through term g_o with units $\mathrm{W/m^3}$, which describes the Joule heating. The centerline of the fluid flow is a zero-flux boundary to represent symmetry. The temperature far upstream and downstream ($x \to \pm\infty$) will be bounded if heating term g_o is applied over a finite region, which we use to represent a heat exchanger of length L.

Green's Function Solution: The geometry described in the previous section involves two regions, the flowing fluid and the adjacent tube wall. Although these regions are quite different, the equations describing the heat transfer in each region differ only by the convection term. That is, the wall equation may be viewed as a special case of the fluid equation with zero convection velocity. With this observation, the solution will be sought using the method of Green's functions applied to multiple discrete concentric layers within the domain, each of which contains a discrete convection velocity. The Green's function is a solution to the same equations and boundary conditions as those satisfied by the temperature, except that the volume heating function $g_o(x)$ is replaced by a point heat source. Then, the temperature

solution is assembled by adding together many Green's functions in such a way that the volume heating function g_o is reconstructed from point sources. This adding together takes the form of superposition integrals, as shown below.

Consider layer i, a typical layer in the domain with inner radius r_{i-1} and outer radius r_i and conductivity k_i. Let $q_{i-1,i}$ be the heat flux entering layer i from the layer below and let $q_{i+1,i}$ be heat flux that enters layer i from the layer above. Refer to Fig. 2. Then, the temperature in layer i may be formally stated in the form of integrals with the method of Green's functions, as follows [12, chap. 3]:

$$\begin{aligned} T_i(x,r) = \frac{1}{k_i}\int q_{i-1,i}(x')G_i(x-x',r,r_{i-1})2\pi r_{i-1}dx' \\ + \frac{1}{k_i}\int q_{i+1,i}(x')G_i(x-x',r,r_i)\,2\pi r_i\,dx' \\ + \frac{1}{k_i}\int g_i(x')\int G_i(x-x',r,r')2\pi r'dr'dx' \end{aligned} \quad (8)$$

There are three integral terms, one each for boundary heat flux and one for internal generation g_i. Internal generation g_i is at most a function of position x, because we assume that internal heating is spatially uniform across the thickness of layer i (this assumption is consistent with multiple thin layers). Quantity G_i is the Green's function (GF) that is evaluated at locations appropriate for each integral term. Assume for the moment that the Green's function is known.

Next the Fourier transform will be used to strip away the integrals on x'. The Fourier transform is defined by the following transform pair:

$$\overline{T}_i(r) = \int_{-\infty}^{\infty} T_i(x,r)e^{-j\beta x}dx \quad (9)$$

$$T_i(x,r) = \frac{1}{2\pi}\int_{-\infty}^{\infty} \overline{T}_i(r)e^{j\beta x}d\beta \quad (10)$$

Apply the Fourier transform to Eq. (4)

$$\begin{aligned} \overline{T}_i(r) = \frac{1}{k_i}\overline{q}_{i-1,i}\,\overline{G}_i(r,r_{i-1})\,2\pi r_{i-1} \\ + \frac{1}{k_i}\overline{q}_{i+1,i}\,\overline{G}_i(r,r_i)\,2\pi r_i \\ + \frac{1}{k_i}\overline{g}_i\int \overline{G}_i(r,r')\,2\pi r'\,dr' \end{aligned} \quad (11)$$

Note that the convolution rule strips away the integrals over x'. The dependence on wave number β has been suppressed to streamline the notation. Quantity $\overline{G}_i$, the Fourier-space GF for a typical layer, is given in [12, p 337]. The above form of the temperature will next be used to construct solutions for the heat fluxes across the interfaces between layers.

Multilayer Solution: The calculation of the heat transfer in the fluid flow and in the adjacent wall is carried out by discretizing the fluid velocity distribution into a collection of concentric layers, each one sliding over its neighbors with piecewise constant velocity. Briefly, the method begins by evaluating the temperature in each layer at the layer interfaces, as a function of the (initially unknown) interface heat fluxes. Suitable matching conditions at each interface are used to construct a set of algebraic equations for the unknown heat fluxes at each layer interface. The heat fluxes are found from a matrix solution. Once the heat fluxes are found, the temperature in any layer is given by Eq. (8). For a full discussion of the layered approach applied to parallel-plate flow see [13].

NUMERICAL CONSIDERATIONS

Some care was needed to obtain efficient evaluation of the Fourier-inversion integral in

Eq. (6), which is an improper integral (limits at infinity). This integral was replaced by a summation of proper integrals, each of fixed width and computed by a standard numerical integration scheme, beginning at $\beta = 0$. Additional terms of this series were added until the fractional change in the magnitude of the running sum was less than a tolerance to provide 4-digit precision. All the coding was carried out with variables of type double-precision complex in Fortran 95. For some situations, large values of β were required in the inverse-transform integral. To avoid numerical overflow in these situations, special exponentially-scaled forms of the Bessel functions were substituted for large arguments [14]. A check on the numerical results was provided by comparison with fully-developed heat transfer in the circular tube for slug flow and for laminar flow [15]. Ten layers in the fluid were sufficient to provide three-digit agreement with the exact solution for laminar flow.

RESULTS AND DISCUSSION

Results were carried out for water flow through metal thick-walled tubes. Wall properties for stainless steel, nickel, aluminum, and copper were used. Wall thickness of $(r_w - r_f)/r_f = 0.5,\ 1.0,\ 2.0,\ 3.0$ were studied. Dimensionless temperature is plotted against the dimensionless axial location. The heating section starts at $x/r_f = 0$ and ends at $x/r_f = 200$ Dimensionless temperature is defined as:

$$T^+ = \frac{(T - T_o)2\pi Lk}{Q}, \tag{12}$$

where Q is the power delivered to the tube:

$$Q = g_o\pi(r_w^2 - r_f^2)L. \tag{13}$$

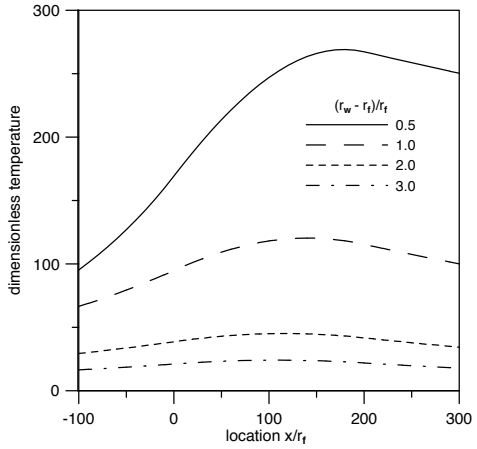

(a) $Pe = 1.0$

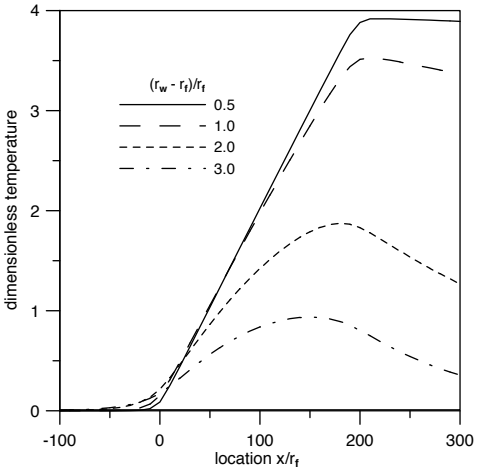

(b) $Pe = 100$

Figure 2
Dimensionless bulk fluid temperature for water flow in a Nickel microtube

Fig. 2 shows the dimensionless bulk fluid temperature for water flow in a Nickel microtube for different Pe and wall thicknesses. As the wall thickness increases the temperature drops due to scaling of the temperature. For the thickest case in Fig. 2–(a), the temperature distri-

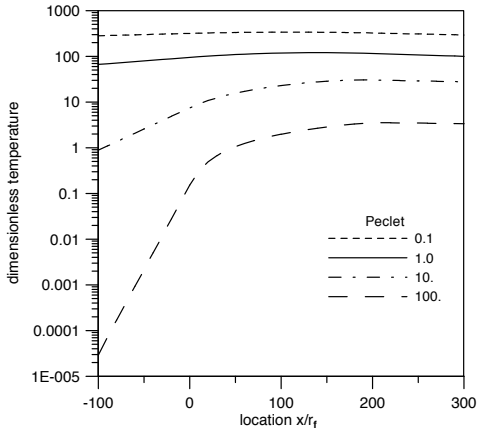

Figure 3
Dimensionless bulk fluid temperature for water flow in a Nickel microtube for different Pe $((r_w - r_f)/r_f = 1.0)$

bution is almost symmetric along tube which indicates the conduction dominated heat transfer (i.e. majority of the heat transfer occurs in the tube wall). As the wall thickness decreases, the symmetry of the temperature breaks down and the domination of the convection can be observed. As Pe increases, the convection dominates and the temperature profile is no more symmetric. Moreover, for thick wall still a maxima in temperature is observed due to the presence of the volumetric heating. As the wall becomes thinner, the difference between the downstream temperature and the maximum temperature decreases and eventually for the thin-walled tube, maximum temperature disappears. Due to the conduction dominates nature of the heat transfer in Case–(a), the heat is transferred in upstream and downstream directions, which causes the heating of the upstream. However, in Case–(b), the upstream is not heated, and all temperature curves start from zero.

To show the effect of the Pe more apparently, Fig. 3 shows the dimensionless bulk fluid temperature for water flow in a Nickel tube for different Pe for fixed wall thickness $((r_w - r_f)/r_f = 1.0)$. For low Pe, the conduction within the fluid and the wall dominates the heat transfer, and since conduction in upstream and downstream direction, the temperature of the starting point of the heating section, the temperature is not zero, which means upstream is heated significantly. As Pe increases, the convection dominates the heat transfer, and now heat is transported in the downstream. The temperature of the starting point of the heating section drops to zero.

Fig. 4 shows the dimensionless bulk temperature for water flow in different microtubes. Different tube materials namely nickel ($k_{wall}/k_{water} = 33$), stainless steel ($k_{wall}/k_{water} = 144$), aluminum ($k_{wall}/k_{water} = 337$) and copper ($k_{wall}/k_{water} = 655$) are shown in the figure. For low Pe, for the materials with higher k, the dominant heat transfer mechanism is the conduction which causes the symmetric temperature distribution. However, for the fixed Pe as the thermal conductivity of the tube decreases, the convection starts to dominate the heat transfer. For higher $Pe = 100$, the effect of the convection can be depicted from the broken symmetry of the temperature. However, still the effect of the volumetric heat generation is present as the maximum point of the temperature exists within the heating section.

CONCLUDING REMARKS

The effect of the volumetric heat generation within the wall of a microtube is investigated.

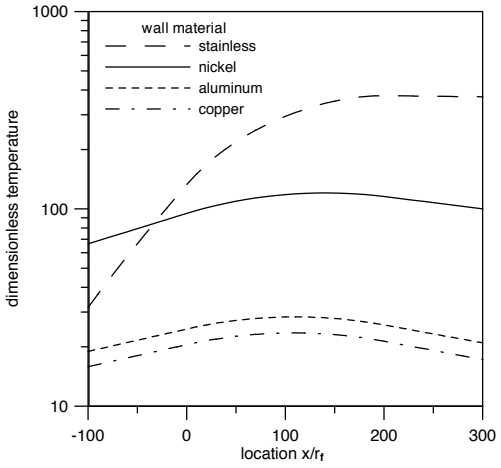

(a) $Pe = 1.0$

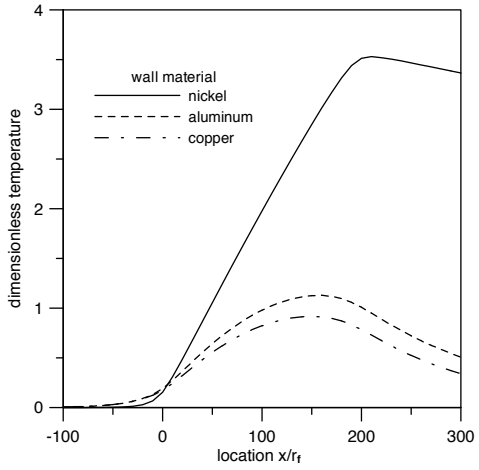

(b) $Pe = 100$

Figure 4
Dimensionless bulk fluid temperature for water flow in different microtubes at fixed all thickness, $(r_w - r_f)/r_f = 1.0$

The heat conduction on the tube wall and in the fluid is considered by extending the solution domain to infinity at both ends. Dimensionless bulk fluid temperature in the microtube is plotted for different Pe, wall thicknesses and wall materials. In this study, a constant volumetric heat generation is assigned within the tube wall. However, in practice the heat generation is generated by means of Joule heating as a result of the applied electric current along the metal tube. To correctly include this effect, calculation of the heat generation due to Joule heating will be performed by the the solution of the Laplace equation within the microtube wall. The inclusion of the heat generation due to Joule heating and the comparison of the results with the available experimental data will be our future research direction.

REFERENCES

1. Cetin, B., 2011. "Effect of thermal creep on heat transfer for a two-dimensional microchannel flow: An analytical approach". *J. Heat Transfer,* **135**(10), p. 101070.

2. Jeong, H. E., and Jeong, J. T., 2006. "Extended Graetz problem including streamwise conduction and viscous dissipation in microchannels". *Int. J. Heat Mass Transfer,* **49**, pp. 2151–2157.

3. Cetin, B., Yazicioglu, A., and Kakac, S., 2008. "Fluid flow in microtubes with axial conduction including rarefaction and viscous dissipation". *Int. Comm. Heat and Mass Transfer,* **35**, pp. 535–544.

4. Cetin, B., Yazicioglu, A., and Kakac, S., 2009. "Slip-flow heat transfer in microtubes with axial conduction and viscous dissipation–An extended Graetz problem". *Int. J. Thermal Sciences,* **48**, pp. 1673–1678.

5. Cetin, B., and Bayer, O., 2011. "Evaluation of Nusselt number for a flow in a microtube using second-order slip model". *Thermal Sciences,* **15 Suppl. 1**, pp. 103–109.

6. Yang, Y., Hong, C., Morini, G. L., and Asako, Y., 2014. "Experimental and numerical investigation of forced convection of subsonic gas flows in microtubes". *Int. J. Heat and Mass Transfer,* **78**, pp. 732–740.

7. Yang, A., Chalabi, H., Lorenzini, M., and Morini, G. L., 2015. "The effect on the nusselt number of the nonlinear axial temperature distribution of gas flows through microtubes". *Heat Transfer Eng.,* **35**(2), pp. 159–170.

8. Goodfellow company-nickel tube material information. `www.goodfellow.com/E/Nickel-Tube.html`. Accessed January 27, 2015.

9. Morini, G. L., 2004. "Single-phase convective heat transfer in microchannels: a review of experimental results". *Int. J. Thermal Sciences,* **43**, pp. 631–651.

10. Barlak, S., Yapc, S., and Sara, O., 2011. "Experimental investigation of pressure drop and friction factor for water flow in microtubes". *Int. J. Thermal Sciences,* **50**, pp. 361–368.

11. Kaya, A., Demiryürek, R., Armağan, E., Ozaydin-Ince, G., Sezen, M., and Kosar, A., 2013. "Boiling heat transfer enhancement in mini/microtubes via polyhydroxyethylmethacrylate (phema) coatings on inner microtube walls at high mass fluxes". *J. Micromech. Microeng.,* **23**, p. 115017.

12. Cole, K. D., Beck, J. V., Haji-Sheikh, A., and Litkouhi, B., 2011. *Heat Conduction Using Green's Functions*, 2 ed. Taylor and Francis, New York.

13. Cole, K. D., and Çetin, B., 2011. "The effect of axial conduction on heat transfer in a liquid microchannel flow". *Int. J. Heat and Mass Transfer,* **54**(11–12), pp. 2542 – 2549.

14. Amos, D. E., and Daniel, S. L., 1974. AMOSLIB Special Function Library, NTIS Technical Report 7503. Tech. rep., Sandia Laboratory Contract AT(29-1)–789.

15. Burmeister, L., 1993. *Convective Heat Transfer*. John Wiley & Sons, p. 128.